New Approach for Calculating Position Domain Integrity Risk for Cycle Resolution in Carrier Phase Navigation Systems

SAMER KHANAFSEH
BORIS PERVAN
Illinois Institute of Technology

A new theoretical approach is described to quantify position-domain integrity risk for cycle ambiguity resolution problems in satellite-based navigation systems. It is typically conservatively assumed that all incorrectly fixed cycle ambiguities cause hazardously large position errors. While simple and practical, this conservative assumption can unnecessarily limit navigation availability for applications with stringent requirements for accuracy and integrity. In response, a new method for calculating the integrity risk for carrier phase navigation algorithms is developed. In this method we evaluate the impact of incorrect fixes in the position domain and define tight upper bounds on the resulting navigation integrity risk. Furthermore, a mechanism to implement this method with partially-fixed cycle ambiguity vectors is also derived. The improvement in navigation availability using the new method is quantified through covariance analysis performed over a range of error model parameters.

Manuscript received July 6, 2008; revised September 22 and October 8, 2008; released for publication October 18, 2008.

IEEE Log No. T-AES/46/1/935943.

Refereeing of this contribution was handled by G. Lachapelle.

This work was supported by the U.S. Navy, Naval Air Warfare Center Aircraft Division (NAWCAD).

This paper is based on a paper presented at the IEEE/ION Position, Location and Navigation Symposium (PLANS 2008), Monterey, CA, May 2008.

Authors' address: Illinois Institute of Technology, MMAE, 10W 32nd St., Rm. 243, Chicago, IL 60616, E-mail: khansam1@iit.edu).

I. INTRODUCTION

Accuracy and integrity risk are fundamental performance measures that affect navigation system availability. In global navigation satellite systems (GNSS), integrity risk is quantified as the probability that the position error exceeds predefined alert limits. For life-critical GNSS applications, such as civil aircraft landing with a ground based augmentation system (GBAS), extremely high levels of integrity are required: integrity risk on the order of 10^{-9} per aircraft approach with a vertical position alert limit of 10 m. However, the accuracy requirements for the GBAS application (vertical 95% accuracy on the order of 2 m) are not stringent enough to require use of high precision carrier phase navigation [1]. This situation is in direct contrast with high accuracy geodetic survey applications, which require carrier phase measurements to achieve centimeter level nominal positioning performance, but otherwise have minimal integrity requirements. However, with the emergence of new aviation applications such as autonomous airborne refueling [2, 3] and autonomous shipboard landing [4, 5], where the life of pilots is involved and the vehicles are highly dynamic, high levels of both integrity and accuracy are required simultaneously. In these situations, the use of carrier phase measurements becomes necessary.

To achieve centimeter level positioning accuracy using carrier phase measurements, cycle ambiguities must be resolved. Over the last two decades, a multitude of research has been conducted in the area of cycle resolution and many different approaches have been developed to fix ambiguities. A summary of the most frequently used methods is provided in [6]. Using some of these methods, it is also possible to provide an a priori measure of the probability of correct cycle estimation. This probability, which is referred to as the probability of correct fix (PCF), must comply with the integrity risk requirements. In applications where integrity and accuracy requirements are stringent, the cycle resolution problem is very challenging.

In a method that has been used previously in such applications to account for cycle resolution integrity risk [7], a threshold on the probability of incorrect fix (PIF) is defined. The PIF threshold must be allocated from, and be smaller than, the allowable overall navigation integrity risk. During a typical navigation operation, only a subset of ambiguities (or linear combinations thereof) can be fixed with a joint incorrect fix (IF) probability lower than the threshold PIF. The rest must be left as real numbers. This set of partially fixed ambiguities is then used in position estimation and to generate the corresponding position domain protection levels. A protection level is a statistical bound for

position error consistent with the allowable overall integrity risk; it is compared with a predefined position domain alert limit for the specific navigation operation. However, in this existing approach it is implicitly and conservatively assumed that all incorrect integer ambiguity candidates will cause the position estimate errors to exceed the alert limits. Unfortunately, fixing a sufficient number of ambiguities to meet the tight accuracy requirements with a success rate that meets the integrity risk requirement is not always possible [8]. In response, a new approach is developed here to calculate integrity risk by evaluating the impact of the incorrect integer candidates directly in the position domain. In addition, a mechanism to implement this method with a partially fixed solution in a navigation system is described.

The availability of carrier phase relative navigation can be greatly enhanced by increasing the PIF threshold [9]. However, as noted above, this probability is bounded by the integrity risk requirement. In this paper, we first revisit the previously used method (briefly described above) where the PIF threshold is conservatively derived from the integrity risk requirement. Next, a theoretical derivation for a tighter upper bound on the integrity risk of ambiguity fix is formulated probabilistically, in which the effect of different sets of ambiguity candidates on the position error is evaluated. To further improve the performance using the new method, we introduce a strategy to obtain partially fixed solutions. In this approach, a subset of ambiguities is fixed only if the resulting position domain integrity risk meets the requirements. The performance of the new method is initially quantified based on a simple geometry test-case. This is followed by an example application of the method to an autonomous shipboard landing navigation problem. Availability analysis over a wide range of error model parameters is then conducted to quantify the performance of the new method for this application.

II. RELATIONSHIP BETWEEN PIF THRESHOLD AND POSITION DOMAIN PROTECTION LEVELS

This section presents the conventional method that has been derived in [7] which provides a formula for the relation between the PIF, threshold, fault-free integrity requirement ($I_{H0\text{req}}$) and the vertical protection level (VPL). To derive such a formula, it is easiest to start with the concept of the fault-free VPL (VPL_{H0}). VPL_{H0} is defined as a statistical overbound where the probability of the vertical position estimate error ($|\hat{x}_v - x_v|$) exceeding VPL_{H0} equals $I_{H0\text{req}}$ (1).

$$P\{|\hat{x}_v - x_v| > \text{VPL}_{H0}\} = I_{H0\text{req}} \tag{1}$$

where

$P\cdot$ is the probability of event '$\cdot$'
$\hat{x}_v$ is the vertical component of the estimated relative position vector
x_v is the vertical component of the true relative position vector

After fixing the ambiguities, two mutually exclusive and exhaustive events can be defined in relation to (1): a correct fix (CF) and an IF event. An IF includes all events where some or all ambiguities have been fixed incorrectly. A CF, on the other hand, includes only those events where no ambiguities are fixed incorrectly. Note that by the definition of a correct fix, if we choose not to fix any ambiguity, thereby leaving the cycle ambiguities floating, then the PCF is equal to 1. At the same time, if we choose to fix some or all ambiguities, we expect PCF to be less than 1. Using the law of total probability, (1) can be expanded to

$$\begin{aligned} &P\{|\hat{x}_v - x_v| > \text{VPL}_{H0}\} \\ &\quad = P\{|\hat{x}_v - x_v| > \text{VPL}_{H0} \mid \text{CF}\}\text{PCF} \\ &\qquad + P\{|\hat{x}_v - x_v| > \text{VPL}_{H0} \mid \text{IF}\}\text{PIF}. \end{aligned} \tag{2}$$

Given that the cycle ambiguities are fixed incorrectly, the probability that the vertical error exceeds VPL_{H0} (i.e., $P\{|\hat{x}_v - x_v| > \text{VPL}_{H0} \mid \text{IF}\}$) can conservatively be assumed to be equal to 1. This assumption is considered conservative because in reality there might be IF events which result in a small vertical error such that $P\{|\hat{x}_v - x_v| > \text{VPL}_{H0} \mid \text{IF}\}$ is less than 1.

Since the CF and IF events are mutually exclusive and exhaustive as defined earlier, PCF = 1 − PIF. Using the conservative assumption $P\{|\hat{x}_v - x_v| > \text{VPL}_{H0} \mid \text{IF}\} = 1$ in (2) and substituting the result in (1),

$$\begin{aligned} I_{H0\text{req}} &= P\{|\hat{x}_v - x_v| > \text{VPL}_{H0} \mid \text{CF}\}\text{PCF} + \text{PIF} \\ &\Rightarrow P\{|\hat{x}_v - x_v| > \text{VPL}_{H0} \mid \text{CF}\} = \frac{I_{H0\text{req}} - \text{PIF}}{1 - \text{PIF}}. \end{aligned} \tag{3}$$

Under the assumption that the GPS measurement noise is zero-mean Gaussian, the vertical position error, after fixing the cycle ambiguities correctly, can be assumed to be a random variable with a Gaussian distribution of zero mean and standard deviation $\sigma_{v|\text{CF}}$. Therefore, a probability multiplier ($K_{\text{VPL}|\text{CF}}$) is calculated using the inverse of the cumulative normal distribution function of $P\{|\hat{x}_v - x_v| > \text{VPL}_{H0} \mid \text{CF}\}$. For example, for $I_{H0\text{req}} = 10^{-7}$, in [7] a reasonable threshold for PIF was found to be 10^{-8}, which results in $K_{\text{VPL}|\text{CF}} = 5.35$. In this case, VPL_{H0} is calculated by multiplying $\sigma_{v|\text{CF}}$ by 5.35. This VPL_{H0} must comply with the maximum tolerable vertical error, which is known as the vertical alert limit (VAL).

If a tighter accuracy and integrity requirement exists, as we examine later in Section V, this method is not sufficient to meet typical navigation availability requirements. One venue to improve the VPL_{H0} calculation is the conservative assumption, made after (2), that all incorrect integer candidates will cause the position errors to exceed the alert limits. In response, in the following section we introduce an innovative approach to calculate the integrity risk by evaluating the impact of the incorrect integer candidates, weighted by their probability of occurrence, in the position domain.

III. POSITION DOMAIN INTEGRITY RISK OF AMBIGUITY FIX

Instead of using the conservative assumption that the vertical error exceeds VPL_{H0} if ambiguities are fixed incorrectly, we consider an integer space that includes all candidate sets of cycle ambiguities that cause the position error to fall inside the alert limit boundaries. This includes all sets, CF or IF, as long as they cause the vertical error to be bounded by the alert limits with the allowable level of integrity risk. In other words, if a candidate set is incorrect but satisfies the position domain alert limit constraints, we recognize that it does not violate integrity.

A. Mathematical Derivation

In this new method, instead of starting from the definition of VPL_{H0} that meets the integrity requirements, we directly calculate the integrity risk (I_{H0}) caused by the cycle ambiguity candidates and compare it with the required fault-free integrity risk ($I_{H0\,\mathrm{req}}$). If the calculated integrity risk (I_{H0}) is less than the required integrity risk then the navigation system is considered available under fault-free conditions. Fault-free integrity risk is defined as the probability that the vertical error exceeds VAL as shown in (4).

$$I_{H0} = P\{|\hat{x}_v - x_v| > \mathrm{VAL}\}. \tag{4}$$

Considering the two mutually exclusive and exhaustive events IF and CF and using the law of total probability as shown in (2), (4) can be rewritten as

$$\begin{aligned} I_{H0} = {} & P\{|\hat{x}_v - x_v| > \mathrm{VAL} \mid \mathrm{CF}\}\mathrm{PCF} \\ & + P\{|\hat{x}_v - x_v| > \mathrm{VAL} \mid \mathrm{IF}\}\mathrm{PIF}. \end{aligned} \tag{5}$$

The second term in the right-hand side of (5) can be expanded to include all possible events that correspond to incorrectly fixed cycle ambiguity vector candidates (6).

$$\begin{aligned} & P\{|\hat{x}_v - x_v| > \mathrm{VAL} \mid \mathrm{IF}\}\mathrm{PIF} \\ & \quad = \sum_{n=1}^{\infty} P\{|\hat{x}_v - x_v| > \mathrm{VAL} \mid \mathrm{IF}_n\}\mathrm{PIF}_n \end{aligned} \tag{6}$$

where

IF_n is the event corresponding to the nth incorrectly fixed cycle ambiguity vector
PIF_n is the probability of occurrence of the nth incorrect fix.

Since it is impractical to calculate the series with an infinite number of incorrect cycle ambiguity vector candidates, the series is broken into two subseries: one represents what will later be the candidates of interest ($n = 1 \rightarrow k$) and another which includes all remaining candidates ($n = k + 1 \rightarrow \infty$) as shown in (7).

$$\begin{aligned} & P\{|\hat{x}_v - x_v| > \mathrm{VAL} \mid \mathrm{IF}\}\mathrm{PIF} \\ & \quad = \sum_{n=1}^{k} P\{|\hat{x}_v - x_v| > \mathrm{VAL} \mid \mathrm{IF}_n\}\mathrm{PIF}_n \\ & \qquad + \sum_{n=k+1}^{\infty} P\{|\hat{x}_v - x_v| > \mathrm{VAL} \mid \mathrm{IF}_n\}\mathrm{PIF}_n. \end{aligned} \tag{7}$$

In order to avoid calculating the second term in (7), the conservative assumption $P\{|\hat{x}_v - x_v| > \mathrm{VAL} \mid \mathrm{IF}_n\} = 1$ for $n = k + 1 \rightarrow \infty$ is used. In addition, since the correct fix event and all incorrect fix events (including the tested candidates) are mutually exclusive and exhaustive, the second term in (7) can be written as

$$\sum_{n=k+1}^{\infty} \mathrm{PIF}_n = 1 - \mathrm{PCF} - \sum_{n=1}^{k} \mathrm{PIF}_n. \tag{8}$$

Substituting (8) into (7) and using the result in (5) yields

$$\begin{aligned} I_{H0} = {} & P\{|\hat{x}_v - x_v| > \mathrm{VAL} \mid \mathrm{CF}\}\mathrm{PCF} \\ & + \sum_{n=1}^{k} P\{|\hat{x}_v - x_v| > \mathrm{VAL} \mid \mathrm{IF}_n\}\mathrm{PIF}_n \\ & + 1 - \mathrm{PCF} - \sum_{n=1}^{k} \mathrm{PIF}_n. \end{aligned} \tag{9}$$

Rearranging (9), we obtain

$$\begin{aligned} I_{H0} = {} & 1 - (1 - P\{|\hat{x}_v - x_v| > \mathrm{VAL} \mid \mathrm{CF}\})\mathrm{PCF} \\ & - \sum_{n=1}^{k} (1 - P\{|\hat{x}_v - x_v| > \mathrm{VAL} \mid \mathrm{IF}_n\})\mathrm{PIF}_n. \end{aligned} \tag{10}$$

Equation (10) is a closed-form expression in which the effect of a set of ambiguity candidates on the position domain integrity risk is explicitly defined. It is noteworthy that if the series term in (10) (which represents the IF candidates to be tested) is neglected, the remaining expression yields

$$\begin{aligned} I_{H0} & = 1 - (1 - P\{|\hat{x}_v - x_v| > \mathrm{VAL} \mid \mathrm{CF}\})\mathrm{PCF} \\ & = \mathrm{PIF} + P\{|\hat{x}_v - x_v| > \mathrm{VAL} \mid \mathrm{CF}\}\mathrm{PCF} \end{aligned} \tag{11}$$

which is equivalent to (3) with VAL and I_{H0} replacing VPL_{H0} and $I_{H0\mathrm{req}}$, respectively. Therefore, as long as the sum of the series in (10) is greater than zero (always true), the integrity risk computed using (10) will be lower than that given by (11). Therefore, (10) provides a tighter bound on integrity risk than the conventional method expressed in (11). This in turn will result in improved navigation availability as we see later in Sections IIIE and V.

In order to compute the integrity risk using (10), the terms PCF, PIF_n, $P\{|\hat{x}_v - x_v| > \mathrm{VAL} \mid \mathrm{CF}\}$, and $P\{|\hat{x}_v - x_v| > \mathrm{VAL} \mid \mathrm{IF}_n\}$ must be evaluated. For compactness of notation, the latter two terms are referred to as P_{VALCF} and P_{VALIF}, respectively. In the following sections, the procedure to compute PCF, PIF, P_{VALCF}, and P_{VALIF} is described. In addition, an efficient method to construct cycle ambiguity candidates is developed.

B. Evaluating PCF and PIF

Calculating the probability that a certain set of ambiguities is the correct one depends on the fixing method utilized. In this work, the bootstrap method [10] is used for cycle resolution because it provides a closed-form a priori probability mass function on integer estimation error. The bootstrap rounding method fixes ambiguities sequentially and provides a measure of the PCF at each step of the fixing process. The sequential adjustment is performed according to the cycle ambiguity conditional variances with the ambiguity having the lowest conditional variance being fixed first. The ith conditional variance ($\sigma^2_{i/I}$), defined as the variance of the ambiguity i conditioned on the previous ambiguities in the set $I = \{1,2,\ldots,i-1\}$ being fixed, is the (i,i) element of the diagonal matrix $\mathbf{D}$ resulting from the $\mathbf{LDL}^T$ decomposition of the floating cycle ambiguity estimate error covariance matrix. At each step in this sequence (the mth step for example), the probability that the bootstrapped integer estimate ($\breve{\mathbf{a}}$) (which is an $m \times 1$ vector) being any arbitrary integer candidate ($\mathbf{z}$) given that the correct fixed ambiguity is ($\mathbf{a}$) is given in [10] as

$$P(\breve{\mathbf{a}} = \mathbf{z}) = \prod_{i=1}^{m} \left[\Phi\left(\frac{1 - 2\mathbf{l}_i^T(\mathbf{a}-\mathbf{z})}{2\sigma_{i/I}} \right) + \Phi\left(\frac{1 + 2\mathbf{l}_i^T(\mathbf{a}-\mathbf{z})}{2\sigma_{i/I}} \right) - 1 \right] \tag{12}$$

where

$\mathbf{l}_i$ is the ith column vector of the unit lower triangular matrix ($\mathbf{L}^{-T}$) resulting from $\mathbf{LDL}^T$ decomposition of the ambiguity covariance matrix,
m is the number of cycle ambiguities fixed $m \leq n$,
$\Phi(x) = \int_{-\infty}^{x} (1/\sqrt{2\pi}) \exp\left(-\frac{1}{2}v^2\right) dv$.

Therefore, if we set $\mathbf{z}$ equal to $\mathbf{a}$ (the correct cycle ambiguity vector), (12) produces

$$P(\breve{\mathbf{a}} = \mathbf{a}) = \prod_{i=1}^{m} \left[2\Phi\left(\frac{1}{2\sigma_{i/I}} \right) - 1 \right] \tag{13}$$

which can be used to calculate PCF. For PIF, the value of $(\mathbf{a}-\mathbf{z})$ can be computed for the IF candidate of interest. For example, if a one cycle error on the first ambiguity is to be used as the first IF event (IF_1), then the vector $[1\ \ 0 \ldots 0]^T$ is used for $(\mathbf{a}-\mathbf{z})$.

C. Evaluating P_{VALCF} and P_{VALIF}

Before estimating the probability of the vertical error exceeding VAL, for simplification purposes and without the loss of generality, the conditional events CF and IF_n are replaced by a general event B. Later on, when we derive a methodology for estimating this probability, we will tackle the difference between the CF and IF events and discuss the specific approach for each one.

By expanding the absolute value inside the conditional probability term of (10), the probability of the vertical error exceeding VAL given that event B took place can be written as

$$P\{|\hat{x}_v - x_v| > \mathrm{VAL} \mid B\} = P\{(\hat{x}_v - x_v) < -\mathrm{VAL} \mid B\} + P\{(\hat{x}_v - x_v) > \mathrm{VAL} \mid B\}. \tag{14}$$

The position vector is linearly estimated using the GPS measurements which are assumed to have Gaussian error distributions with zero mean. Therefore, the distribution of the vertical position estimate error would also be Gaussian with a standard deviation defined as $\sigma_{v|B}$. The mean of this distribution will depend on the event B and hence is referred to as μ_B. Knowing the mean (μ_B) and the standard deviation ($\sigma_{v|B}$), the probability of the first and second terms of (14) can be calculated using the normal cumulative distribution function at the limits $-\mathrm{VAL}$ and VAL, respectively.

Returning to the CF and IF_n events, the standard deviation of the vertical position error is not affected by an IF. Therefore, $\sigma_{v|B} = \sigma_{v|\mathrm{CF}}$ for both the CF and IF_n events. The calculation of $\sigma_{v|\mathrm{CF}}$ is detailed in Appendix A. The only difference between these events is the mean of the Gaussian distribution. Since the position vector is estimated using unbiased estimators (usually least squares or Kalman filter estimation is used), the mean is zero for the CF event ($\mu_{\mathrm{CF}} = 0$). In the case of IF_n events, the incorrect integer candidate will induce a bias in the position vector estimate. The bias $\mathbf{b}_n$ induced in the relative position vector caused by the nth $(a-z)_n$ incorrect candidate is derived in Appendix A and can be computed as

$$\mathbf{b}_n = \mathbf{K}(\mathbf{a}-\mathbf{z})_n \tag{15}$$

where $\mathbf{K} = \mathbf{P}[\mathbf{0}_{n\times 3}\ \mathbf{Z}_{1:n}]^T([\mathbf{0}_{n\times 3}\ \mathbf{Z}_{1:n}]\mathbf{P}[\mathbf{0}_{n\times 3}\ \mathbf{Z}_{1:n}]^T)^{-1}$, $\mathbf{P}$ is the position and float ambiguities state estimate error covariance, and $\mathbf{Z}_{1:n} = [\mathbf{I}_{n\times n}\ \mathbf{0}_{n\times(m-n)}]$ with m being the total number of states.

P_{VALIF} can be then calculated using a normal cumulative distribution function with standard deviation $\sigma = \sigma_{v|\text{CF}}$ and a mean ($\mu_{\text{IF}n} = \mathbf{b}_n$) where $\mathbf{b}_n$ is calculated using (15).

If requirements other than VAL, such as lateral alert limit (LAL), vertical accuracy (Acc_v) or lateral accuracy (Acc_L) exist, (10) can be altered accordingly. Equations (16), (17), and (18) show the corresponding form of (10) for LAL, vertical and lateral accuracy requirements, respectively.

$$I_{H0\text{LAL}} = 1 - (1 - P\{|\hat{x}_L - x_L| > \text{LAL} \mid \text{CF}\})\text{PCF} - \sum_{n=1}^{k}(1 - P\{|\hat{x}_L - x_L| > \text{LAL} \mid \text{IF}_n\})\text{PIF}_n \tag{16}$$

$$P_{\text{acc}V} = 1 - (1 - P\{|\hat{x}_v - x_v| > \text{Acc}_v \mid \text{CF}\})\text{PCF} - \sum_{n=1}^{k}(1 - P\{|\hat{x}_v - x_v| > \text{Acc}_v \mid \text{IF}_n\})\text{PIF}_n \tag{17}$$

$$P_{\text{acc}L} = 1 - (1 - P\{|\hat{x}_L - x_L| > \text{Acc}_L \mid \text{CF}\})\text{PCF} - \sum_{n=1}^{k}(1 - P\{|\hat{x}_L - x_L| > \text{Acc}_L \mid \text{IF}_n\})\text{PIF}_n \tag{18}$$

where

$I_{H0\text{LAL}}$ is the lateral fault free integrity risk,
Acc_v is the vertical accuracy requirement,
$P_{\text{acc}V}$ is the probability that the vertical position error exceeds Acc_v,
Acc_L is the lateral accuracy requirement,
$P_{\text{acc}L}$ is the probability that the lateral position error exceeds Acc_L.

Furthermore, (10) can also be used to provide a tight overbound for VPL_{H0} if required by replacing I_{H0} and VAL with $I_{H0\text{req}}$ and VPL_{H0}, respectively, as shown in (19):

$$I_{H0\text{req}} = 1 - (1 - P\{|\hat{x}_v - x_v| > \text{VPL}_{H0} \mid \text{CF}\})\text{PCF} - \sum_{n=1}^{k}(1 - P\{|\hat{x}_v - x_v| > \text{VPL}_{H0} \mid \text{IF}_n\})\text{PIF}_n \tag{19}$$

where VPL_{H0} can be computed iteratively, using a Newton-Raphson method for example.

Special care should be taken if any lateral requirements exist. In nominal GPS applications the vertical accuracy is usually worse than the lateral accuracy because of the geometry of the satellites (satellites are visible above the horizon only) and its correlation with the receiver clock error. However in the case of incorrect fixing, position biases might exist at different magnitudes and in different directions. Under IF conditions, it is quite possible to find a few cases under which the vertical requirements are met while the lateral ones are not.

In most navigation applications, the lateral requirements are defined perpendicular to the flight path. Since the geometry of the satellites generally produces different errors in the North and East directions, lateral position error depends on the flight path azimuth. To be conservative in calculating availability, the azimuth that produces the worst accuracy shall be used. In the CF case, the worst case lateral error variance is simply the maximum eigenvalue of the (2×2) horizontal position error covariance matrix. However, when biases of different magnitudes and directions are introduced to the North and East directions (as in the case of IF), this is not necessarily the case. An alternative method that shows how to find the worst heading for lateral requirements and how to calculate the associated mean (μ_{IF}) and standard deviation ($\sigma_{L|\text{IF}}$) is detailed in Appendix B.

D. Generating Cycle Ambiguity Candidates

In principle, cycle ambiguity candidates can be constructed by directly considering all possible combinations of cycle errors for all ambiguities. As discussed in Section IIIA, theoretically, if the series term $\sum_{n=1}^{k}(1 - P\{|\hat{x}_v - x_v| > \text{Acc}_v \mid \text{IF}_n\})\text{PIF}_n$ in (10) is negligibly small, in (10) we expect no reduction in the computed integrity risk using the new method compared with the conservative one in (3). The terms in this series will be close to zero under two scenarios: if P_{VALIF} is large (close to 1), or if PIF is small (close to zero). P_{VALIF} will be large if the IF ambiguity candidates introduce large biases (μ_{IF}) in the position domain. On the other hand, from (12) it can be observed that the larger $(\mathbf{a} - \mathbf{z})$ is, which is the case when the incorrectly fixed ambiguity $\mathbf{z}$ is farther from the correct one $\mathbf{a}$ (the one with maximum probability of CF), the smaller PIF becomes. Therefore, adding more candidates with larger $(\mathbf{a} - \mathbf{z})$ will not change the series outcome significantly. Therefore, it is not necessary to search the whole integer space ($k \to \infty$) for IF candidates. It is adequate to use only the ones surrounding the CF ($\mathbf{a}$) that lead to near convergence of the series in (10). Since the fixing process is performed sequentially, the number of IF candidates is expected to grow as the number of fixed ambiguities increases. For example, if IFs of up to 5 cycles in magnitude different from the correct one are to be considered, the number of ambiguity candidates of interest starts from $11^1 - 1 = 10$ (-5 to 5 skipping 0 which represents the CF) when fixing the first ambiguity. In a double difference dual frequency application with eight visible satellites

for example, the number of ambiguities to be fixed is 14 and the number of ambiguity candidates grows up to ($11^{14} - 1 \approx 3.8 \times 10^{14}$). In order to reduce the computation burden of building the IF ambiguity candidates, the following procedure is developed to construct cycle ambiguity candidates more efficiently.

1) Define a candidate matrix ($\mathbf{C}$) as the matrix whose columns represent all the vectors ($\mathbf{a} - \mathbf{z}$) for all incorrectly fixed ambiguity candidates. Since one integer is fixed first, $\mathbf{C}$ is initialized with a row vector of integer numbers representing ($\mathbf{a} - \mathbf{z}$) candidates for the first ambiguity. Therefore, if d is used as an arbitrary integer bound on ($\mathbf{a} - \mathbf{z}$), then $\mathbf{C}_1 = [-d, -d+1, \ldots, -1, 1, \ldots, d-1, d]$. This corresponds to the first step in the bootstrap sequential fixing (fixing one ambiguity only).

2) For each step in the sequential fixing, other than the initial one, update $\mathbf{C}_i$ includes all new combinations for the newly fixed ambiguity. This can be accomplished, for $2 = i = n$, by

$$\mathbf{C}_i = \begin{bmatrix} \mathbf{C}_{i-1}^T & -\mathbf{d} \\ \mathbf{C}_{i-1}^T & -\mathbf{d}-\mathbf{1} \\ \vdots & \vdots \\ \mathbf{C}_{i-1}^T & \mathbf{0} \\ \vdots & \vdots \\ \mathbf{C}_{i-1}^T & \mathbf{d}-\mathbf{1} \\ \mathbf{C}_{i-1}^T & \mathbf{d} \\ \mathbf{0} & -\mathbf{d} \\ \mathbf{0} & -\mathbf{d}+\mathbf{1} \\ \vdots & \vdots \\ \mathbf{0} & -\mathbf{1} \\ \mathbf{0} & \mathbf{1} \\ \vdots & \vdots \\ \mathbf{0} & \mathbf{d}-\mathbf{1} \\ \mathbf{0} & \mathbf{d} \end{bmatrix}^T$$

where $\mathbf{d}$ is a column vector with all of its elements equal to d and $\mathbf{1}$ is a column with all its elements equal to 1.

3) Calculate PIF for each $(\mathbf{a} - \mathbf{z})_i$ candidate (each column of the $\mathbf{C}_i$ matrix).

4) Only the relevant candidates that are significant in the calculation of the series in (10) are kept in $\mathbf{C}$. Therefore, if PIF for the kth candidate (kth column of $\mathbf{C}_i$) is less than a threshold (for example $0.01 \times I_{H0\text{req}}$), then the kth column in $\mathbf{C}_i$ is eliminated.

5) The resultant $\mathbf{C}_i$ is the matrix that includes all ambiguity candidates that are relevant in (10) and will be used in the calculation of I_{H0}.

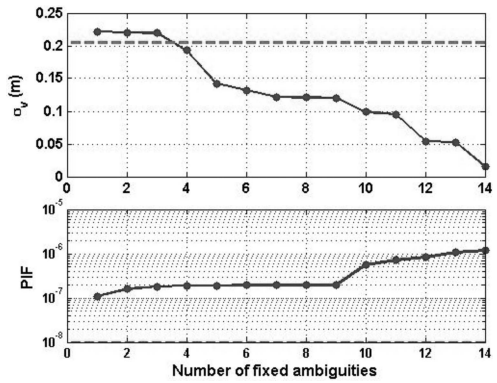

Fig. 1. Vertical accuracy and PIF versus number of fixed ambiguities using conventional method.

6) Steps 2–5 are repeated for all ambiguities ($i \leq n$) necessary to be fixed to meet the requirements.

Although this sequential elimination procedure is general and more efficient than considering all combinations, it still requires a significant amount of memory. However, its efficiency can be greatly enhanced and its computation time can be considerably reduced if the ambiguities to be fixed are decorrelated, for example using the least-square ambiguity decorrelation adjustment (LAMBDA) method [11] or the Hassibi, et al. decorrelation method that was based on the Lenstra, Lenstra, and Lovasz (LLL) algorithm [12]. With prior decorrelation of ambiguities performed using LAMBDA in the examples later in this work, only combinations with $d = 1$ need to be considered (as we will see shortly). Note, however, that when an integer transformation matrix $\mathbf{Z}$ is used to decorrelate the ambiguities, $\mathbf{Z}_{1:m}$ in (15) becomes the rows 1 to m of $\mathbf{Z}$. Also, the $\mathbf{LDL}^T$ decomposition in Section IIIB must be performed on the decorrelated ambiguity matrix.

E. Performance Enhancement using the Position Domain Integrity Risk Method

In order to demonstrate the gain using the position domain integrity risk method (which we refer to as the 'new method' for short) over the conventional method explained in Section II, a simple example for a single measurement epoch is used. In this example, a single satellite geometry consisting of 8 satellites is used to provide the float cycle ambiguity estimates and the corresponding covariance. First we illustrate the performance of the conventional method for this geometry. After estimating fourteen L1/L2 dual frequency double difference float ambiguities (7 ambiguities for L1 and 7 for L2), LAMBDA is used to decorrelate the estimated cycle ambiguity covariance matrix and the bootstrap method is used to sequentially fix the ambiguities. At each step in this sequential fixing process, PCF using (13) and the resultant vertical position accuracy (σ_v) are recorded. In Fig. 1, the vertical accuracy and PIF (where PIF =

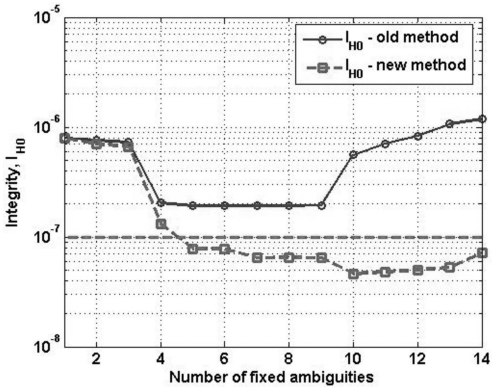

Fig. 2. Integrity as function of number of fixed ambiguities for both conventional method and new method.

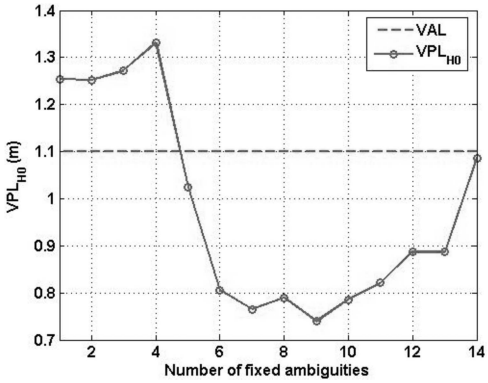

Fig. 3. VPL_{H0} as function of number of fixed ambiguities for both conventional method and new method.

$1 - PCF$) are illustrated versus the number of fixed ambiguities during the sequential fixing. In each of these plots the corresponding thresholds which are derived from certain assumed requirements are also shown as dashed lines. For example, in the σ_v plot the dashed line represents the VAL requirement, which is calculated by dividing the VAL (for example 1.1 m is used here) by $K_{\mathrm{VPL|CF}} = 5.35$ as shown in Section II. For the PIF plot, the dashed line corresponds to the 10^{-8} PIF threshold that is derived from the example integrity risk requirement as explained in Section II. From Fig. 1, it is obvious that although at least four cycle ambiguities must be fixed to meet the VAL requirements, fixing even the first cycle ambiguity violates integrity (shown in the PIF plot). Since both the VAL and integrity risk requirements cannot be met simultaneously, this geometry is considered unavailable using the conventional method of Section II.

The results shown in Fig. 1 can be combined in one plot (solid curve in Fig. 2) that shows integrity I_{H0} calculated using (11) (without the series term) versus the number of fixed ambiguities. If I_{H0} exceeds the integrity risk requirement (for example, $I_{H0\mathrm{req}} = 10^{-7}$), the satellite geometry is considered unavailable. Therefore, the solid curve in Fig. 2 confirms that I_{H0} using the conventional method (11) does not meet the integrity risk requirement for this geometry for any number of fixed ambiguities. However, using the new method in (10), the integrity risk requirement is met if more than four ambiguities are fixed. In addition to I_{H0}, VPL_{H0} was computed iteratively by applying Newton-Raphson method on (19). Fig. 3, which represents VPL_{H0} as the number of fixed ambiguity increases, confirms the results and conclusions for the new method seen in Fig. 2.

Using LAMBDA decorrelation, 108 combinations of one-cycle-off candidates were adequate to generate the results shown in Fig. 2. On the other hand, if LAMBDA decorrelation is not used, incorrect fixes of up to five cycles are necessary, resulting in 1792 candidates. Comparing these numbers with 3.8×10^{14} candidates corresponding to all combinations of five cycles off illustrates the efficiency of the candidate generation procedure described in Section IIID.

Fig. 2 and Fig. 3 show that for the example geometry the values of I_{H0} and VPL_{H0} are higher when all ambiguities are fixed, rather when fewer are fixed (for example, ten). This is an important observation, because for an arbitrary geometry, it may happen that the geometry would be unavailable in the all-fixed case, but would be available if fewer ambiguities are fixed. Therefore, a partial-fix implementation is needed in the general case [13]. A practical method to choose the number of fixed ambiguities that meets the integrity requirement is discussed in the next section.

IV. PARTIAL FIXING USING POSITION DOMAIN INTEGRITY RISK METHOD

In this section, a procedure to determine the navigation system availability using the position domain integrity risk method with partial fixing is described. In the previous section, it was concluded that a partially fixed solution is necessary to improve the availability using the proposed algorithm.

Fig. 4 shows a flow chart that describes the final partial fixing algorithm using a hybrid of the conventional and the new method implementation in a navigation architecture. After estimating the float ambiguities, the float estimates ($\hat{\mathbf{N}}$ in Fig. 4) are input to the LAMBDA bootstrap fixing algorithm. These ambiguities are fixed sequentially until the PIF exceeds the threshold (1×10^{-8}). The remaining linear combinations are left floating. At this point, if the resultant VPL_{H0} is less than VAL then this geometry is available and therefore it is unnecessary to go to the second loop, which contains the position domain integrity calculation. If VPL_{H0} is greater than VAL the IF candidates are then constructed for the set of fixed ambiguities up to this point. Using these candidates, I_{H0} using (10) is calculated and compared

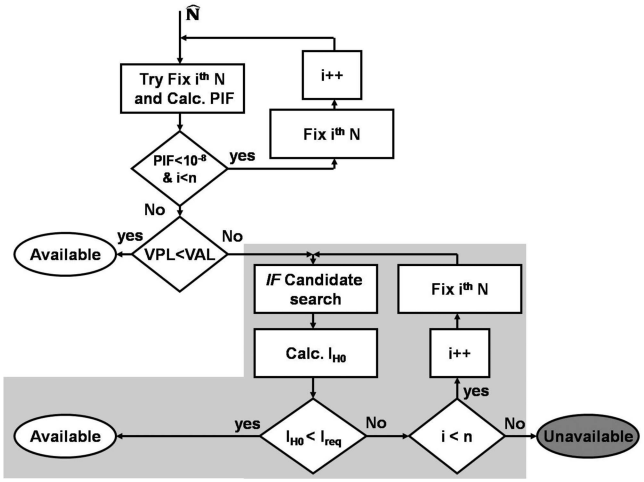

Fig. 4. Schematic diagram showing structure of partial fixing algorithm using position domain integrity of ambiguity fix method.

with the integrity risk requirement $I_{H0\text{req}}$. If I_{H0} is less than $I_{H0\text{req}}$, the geometry is considered available. Otherwise, the next ambiguity is fixed. This process is repeated until an available solution is found or all ambiguities are fixed and I_{H0} is still larger than $I_{H0\text{req}}$. At this point, the geometry is said to be unavailable. Although this process can be repeated to scan through all ambiguities then search for the minimum integrity and fix the corresponding number of ambiguities, this consideration is computationally inefficient. Specifically, from a practical point of view, as long as all requirements are met for a specific application, there is no real necessity in fixing more ambiguities.

So far, the performance enhancement using the new method has been demonstrated based on a single geometry only. In order to investigate the potential for performance benefit more thoroughly, an availability analysis for an example shipboard aircraft landing application is conducted using both the conventional and new methods.

V. AVAILABILITY PERFORMANCE

A. Navigation Algorithm

This section is a description of the navigation architecture in which the developed fixing method described in Section III is implemented. This navigation architecture is designed to support a specific application: autonomous shipboard landing. The outputs of the shipboard-landing navigation architecture (float estimates and their covariance matrices) are used as inputs to the fixing algorithm. Because of the mobility of the reference station in a shipboard-relative landing application, higher levels of accuracy are required than for similar precision approach applications at land-based airfields. In addition, to ensure safety and operational usefulness, the navigation architecture must provide high levels of integrity and availability. Because of the highly stringent requirements, the navigation system is based on carrier phase differential GPS (CPDGPS) positioning. However in order to benefit from the high precision of CPDGPS the correct resolution of cycles must be ensured. A number of methods have been used in prior work to aid in the cycle resolution. Satellite motion can provide the observability of the cycle ambiguities [14]. Unfortunately the rate of satellite motion is relatively slow in comparison with the time scales of the most stringent aviation application such as precision approach and landing.

Heo, et al. have proposed a GPS navigation algorithm for autonomous shipboard landing applications where geometry free/divergence free code-carrier filtering is performed continuously for visible satellites on both the aircraft and the ship until the aircraft is close to the ship [5, 8]. Geometry free filtering [15], by definition, does not depend on the geometry of the satellites or the user location and eliminates all error sources except for receiver noise and multipath. A geometry free measurement of the widelane cycle ambiguity is formed by subtracting the narrowlane pseudo-range from the widelane carrier [14, 15]. A drawback of the geometry free measurement is the presence of higher noise relative to the L1 and L2 carrier phase measurements. This can be overcome by filtering the geometry free measurement over time prior to the final approach. In order to model colored multipath noise in the geometry free measurements, a first-order Gauss-Markov measurement error model is used. A time constant of 1 min for the ship and 30 s for aircraft is assumed. The outputs of the filtering process are the floating widelane cycle ambiguity estimates. When the aircraft is close to the ship, L1/L2 cycle ambiguity estimates can be extracted with the aid of the satellite geometric redundancy [5, 4]. Next, the cycle ambiguities are fixed using the bootstrap method [10]. For the conventional method, the bootstrap rounding process is performed for those ambiguities that can be fixed with a PIF that is lower than a threshold of 10^{-8}. The remaining ambiguities remain floating. With the ambiguities partially fixed, the standard deviation of the position estimate error (σ_v) is used to calculate VPL_{H0}. To account for the GPS satellite geometry change, availability analysis is performed by simulating 1440 satellite geometries (one geometry per minute during the day). Availability is then calculated as the percentage of time (geometries) for which VPL_{H0} is less than VAL. For the new method, the position domain integrity of cycle resolution (I_{H0}) is calculated using (10). If I_{H0} is less than the requirements ($I_{H0\text{req}}$) the geometry is considered available.

TABLE I
Simulation Parameters

Parameter	Value
$I_{H0\,\mathrm{req}}$	10^{-7}
VAL	1.1 m
LAL	1.1 m
PIF threshold	10^{-8}
Satellite constellation	Standard 24 satellite (DO229C) [16]
Location	Honolulu (22°N and 158°W)
Maximum prefiltering time	30 min
Ship multipath time constant	1 min
Aircraft multipath time constant	30 s

B. Availability Results

In this section, the performance of the position domain integrity risk method with partial fixing (Fig. 4) is compared with the conventional method (Section II). The requirements and simulation parameters that are used in this work are based on those given in [5] and [8]. An accuracy requirement of 30 cm with $P_{\mathrm{acc}} = 95\%$ is used to evaluate the effectiveness of the new method under a tighter accuracy requirement than the ones implicitly provided by the alert limits. In this simulation, the standard deviation of the carrier phase (single difference) measurement noise $\sigma_{\Delta\phi}$ is assumed to be 1 cm. In addition, different values for the standard deviation of the pseudo-range (single difference) measurement noise $\sigma_{\Delta\mathrm{PR}}$ ranging from 20 cm to 70 cm are used. The single difference standard deviations $\sigma_{\Delta\mathrm{PR}}$ and $\sigma_{\Delta\phi}$ are related to the raw values (σ_{PR} and σ_{ϕ}) by a scaling factor of $\sqrt{2}$. In this analysis, a maximum prefiltering period of 30 minutes is used to generate floating estimates of the widelane cycle ambiguities. In other words, if the satellite has been visible for a period of time longer than the maximum prefiltering time, the prefiltering time is set to the maximum prefiltering time. The rest of the simulation parameters are summarized in Table I.

Using the parameters detailed in Table I, a covariance analysis simulation was performed and availability was calculated. Fig. 5 shows the availability results for both methods using different $\sigma_{\Delta\mathrm{PR}}$ values ranging from 20 cm to 70 cm. It can be noticed that the new method outperforms the conventional method by a range of approximately 1% at $\sigma_{\Delta\mathrm{PR}} = 20$ cm to as much as 40% at $\sigma_{\Delta\mathrm{PR}} =$ 70 cm. Furthermore, in the case that the availability requirement is 99% (a typical requirement), a navigation algorithm with the conventional method can only be used if $\sigma_{\Delta\mathrm{PR}} = 20$ cm. On the other hand, if the new method is used, $\sigma_{\Delta\mathrm{PR}}$ of up to 55 cm can be tolerated. The results shown in Fig. 5 are for an accuracy requirement of 30 cm. Fig. 6 shows the efficiency of the new method compared with the conventional one for different accuracy requirements using $\sigma_{\Delta\mathrm{PR}} = 50$ cm. Again, the new method outperforms the conventional method and provides up to 78% increase in availability at 15 cm accuracy compared with the conventional one.

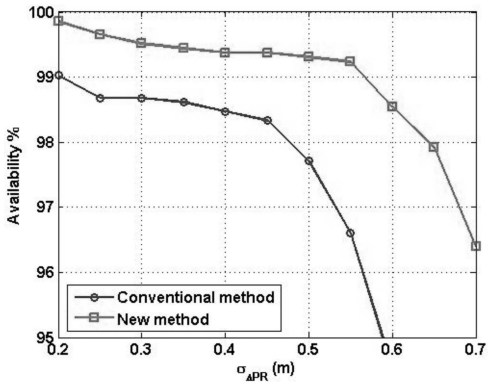

Fig. 5. Availability results for different $\sigma_{\Delta\mathrm{PR}}$ values using both conventional method and new method.

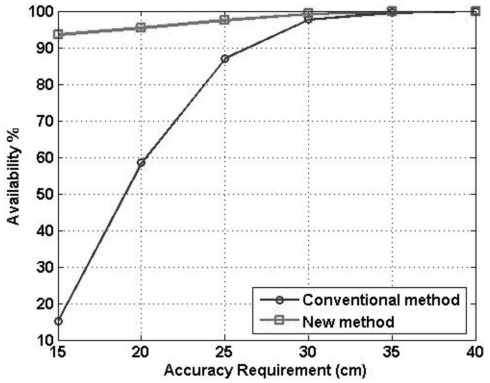

Fig. 6. Availability results for different accuracy requirements using both conventional method and new method at $\sigma_{\Sigma\mathrm{PR}} = 50$ cm.

In summary, the position domain integrity risk method can be greatly beneficial in navigation applications with high accuracy, stringent integrity, and tight availability requirements. Recall that the numerical calculations in this work have been implemented using the bootstrap method. LAMBDA was only used to decorrelate the estimated ambiguity covariance, which increases the computational efficiency but is otherwise not required. However, the integrity risk formulas derived here are equally applicable to other cycle resolution algorithms as long as they are capable of quantifying the probability of fixing on any given integer candidate set.

VI. CONCLUSIONS

A new method was developed to calculate the fault-free integrity risk for cycle resolution in carrier phase navigation algorithms by evaluating the impact of IFs in the position domain. In addition, a mechanism to implement this method with a partially

fixed solution was described. The improvement in navigation availability using this partial fixing method was quantified for an example shipboard landing relative navigation application. The availability analysis demonstrated that the new method provides considerable availability enhancement relative to the existing methods. For the near future, an experimental validation and real time implementation of this method will be considered.

APPENDIX A

This appendix explains how to compute $\sigma_{v|\mathrm{CF}}$ and the position domain bias $\mathbf{b}_n$ induced in the relative position vector caused by the incorrect ambiguity candidates.

Assume that prior to the fixing step, the estimate vector $\hat{\mathbf{S}}$ of the float cycle ambiguities and the relative position vector and the associated estimate error covariance are available as

$$\hat{\mathbf{S}} = \begin{bmatrix} \hat{\mathbf{x}} \\ \hat{\mathbf{N}} \end{bmatrix}$$

and

$$\mathbf{P} = \begin{bmatrix} \mathbf{P}_{\hat{\mathbf{x}}} & \mathbf{P}_{\hat{\mathbf{x}}\hat{\mathbf{N}}} \\ \mathbf{P}_{\hat{\mathbf{N}}\hat{\mathbf{x}}} & \mathbf{P}_{\hat{\mathbf{N}}} \end{bmatrix}.$$

First, the kth ambiguity in the Z-decorrelated space $\hat{N}_z^{(k)}$ is rounded to its nearest integer $N_z^{(k)}$.

$$N_z^{(k)} = \mathrm{round}([\mathbf{0}_{1\times 3} \quad \mathbf{Z}_k]\mathbf{S}^{(k-1)}) \tag{20}$$

where

$N_z^{(k)}$ is the kth rounded ambiguity element,
$\mathbf{Z}_k$ is the kth row of the transformation matrix $\mathbf{Z}$. Notice, however, that if LAMBDA is not used, $\mathbf{Z}_{1:k} = [\mathbf{0}_{1\times(k-1)} \;\; 1 \;\; \mathbf{0}_{1\times(n-k)}]$,
$\mathbf{S}^{(k-1)}$ is the updated state vector $\mathbf{S}$ based on fixing ambiguities 1 to $k-1$, such that $(\mathbf{S}^{(0)} = \hat{\mathbf{S}} = [\hat{\mathbf{x}} \;\; \hat{\mathbf{N}}]^T)$.

Next, the position vector estimate and remaining real valued ambiguities $\mathbf{S}$ are updated accordingly as follows:

$$\mathbf{K} = \mathbf{P}^{(k-1)}[\mathbf{0}_{1\times 3} \quad \mathbf{Z}_k]^T([\mathbf{0}_{1\times 3} \quad \mathbf{Z}_k]\mathbf{P}^{(k-1)}[\mathbf{0}_{1\times 3} \quad \mathbf{Z}_k]^T)^{-1} \tag{21}$$

$$\mathbf{S}^{(k)} = \mathbf{S}^{(k-1)} + \mathbf{K}(N_z^{(k)} - [\mathbf{0}_{1\times 3} \quad \mathbf{Z}_k]\mathbf{S}^{(k-1)}) \tag{22}$$

$$\mathbf{P}^{(k)} = (\mathbf{I} - \mathbf{K}[\mathbf{0}_{1\times 3} \quad \mathbf{Z}_k])\mathbf{P}^{(k-1)} \tag{23}$$

where $\mathbf{P}^{(k)}$ is the covariance of the updated state vector after fixing the kth cycle ambiguity, such that $(\mathbf{P}^{(0)} = \mathbf{P})$. This process is repeated for the desired number of fixed ambiguities (for example m times). At this point, $\sigma_{v|\mathrm{CF}}$ can be computed as the square root of the (3,3) element of $\mathbf{P}^{(m)}$.

$$\sigma_{v|\mathrm{CF}} = \sqrt{\mathbf{P}^{(m)}_{(3,3)}}. \tag{24}$$

For calculating the position domain bias $\mathbf{b}_m$, we start by knowing that the states after fixing m ambiguities (replacing (21) and (22)) by their equivalents:

$$\mathbf{K} = \mathbf{P}[\mathbf{0}_{m\times 3} \quad \mathbf{Z}_{1:m}]^T([\mathbf{0}_{m\times 3} \quad \mathbf{Z}_{1:m}]\mathbf{P}[\mathbf{0}_{m\times 3} \quad \mathbf{Z}_{1:m}]^T)^{-1} \tag{25}$$

$$\mathbf{S}^{(m)} = \hat{\mathbf{S}} + \mathbf{K}(\mathbf{N}_z^{(1:m)} - [\mathbf{0}_{m\times 3} \quad \mathbf{Z}_{1:m}]\hat{\mathbf{S}}) \tag{26}$$

where $\mathbf{Z}_{1:m}$ is the rows 1 to m of the transformation matrix $\mathbf{Z}$. If LAMBDA is not used, $\mathbf{Z}_{1:m}$ is replaced by $\mathbf{Z}_{1:m} = [\mathbf{I}_{m\times m} \;\; \mathbf{0}_{m\times(n-m)}]$.

Now, if we assume that the correct ambiguities vector is $\mathbf{a}_m$ and the incorrect ambiguities vector is $\mathbf{z}_m$, the estimated states become after fixing the ambiguities to the correct ones ($\mathbf{S}_{\mathrm{CF}}$) and the states after fixing the ambiguities to the incorrect ones ($\mathbf{S}_{\mathrm{IF}}$), respectively, are:

$$\mathbf{S}^{(m)}_{\mathrm{CF}} = \hat{\mathbf{S}} + \mathbf{K}(\mathbf{a}_m - [\mathbf{0}_{m\times 3} \quad \mathbf{Z}_{1:m}]\hat{\mathbf{S}}) \tag{27}$$

$$\mathbf{S}^{(m)}_{\mathrm{IF}} = \hat{\mathbf{S}} + \mathbf{K}(\mathbf{z}_m - [\mathbf{0}_{m\times 3} \quad \mathbf{Z}_{1:m}]\hat{\mathbf{S}}). \tag{28}$$

Therefore, the position domain bias $\mathbf{b}_m$ induced in the relative position vector caused by the mth $(a-z)_m$ incorrect candidate is

$$\mathbf{b}_m = \mathbf{S}^{(m)}_{\mathrm{CF}} - \mathbf{S}^{(m)}_{\mathrm{IF}} = \mathbf{K}(\mathbf{a} - \mathbf{z})_m. \tag{29}$$

APPENDIX B

In calculating integrity and availability, worst case scenarios are usually pursued. Using the vertical error component σ_v of the estimated position vector, P_{VAL} can be directly calculated. In contrast, the lateral direction for the LAL is defined as the direction perpendicular to the direction of motion of the vehicle. The relative position vector estimation provides a covariance matrix ($\mathbf{P}$) for the North and East directions, which can be represented as a covariance ellipse. If this covariance ellipse is centered at the origin (zero mean error), the direction of the major axis of this ellipse represents the direction (heading) corresponding to the maximum sigma lateral (σ_L). Therefore, in the case of a CF, the worst P_{LALCF} is based on σ_L which is the square root of the maximum eigenvalue of the 2×2 covariance matrix of the position vector estimate error. However, in the IF case, biases in the North and East directions (μ_n and μ_e) are introduced. Therefore, the covariance ellipse is centered at (μ_e, μ_n) instead of the origin (Fig. 7). As a result, the direction of the major axis will not necessarily correspond to the worst P_{LALIF}. In this work, all heading angles (θ) from 1 to 360 deg (in 1 deg increments) are considered and $P_{\mathrm{LAL}}(\theta)$ is computed for all θ. The maximum value of $P_{\mathrm{LAL}}(\theta)$ is chosen as P_{LALIF}.

In order to calculate the mean (μ) and standard deviation (σ_L) that are used in calculating P_{LALIF}, a coordinate rotation by angle θ is performed on the

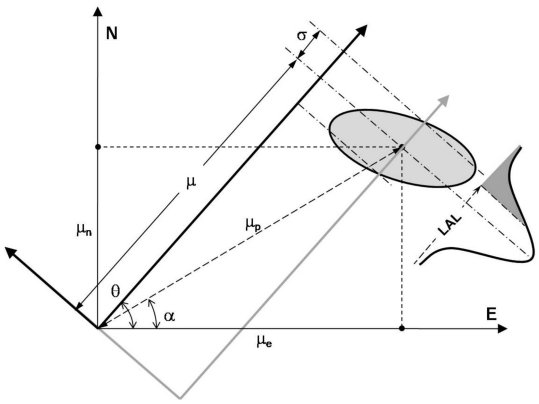

Fig. 7. Calculating mean and standard deviation of projection of covariance ellipse for heading angle θ.

covariance ellipse. This can be performed by first computing the position mean magnitude (μ_p) and the direction of the mean (α) as follows:

$$\mu_p = \sqrt{\mu_n^2 + \mu_e^2}$$
$$\alpha = \tan^{-1}\left(\frac{\mu_n}{\mu_e}\right). \tag{30}$$

Therefore, the projection of the mean on the new direction, which is the mean that is used in calculating LAL, is

$$\mu = \mu_p \cos(\theta - \alpha). \tag{31}$$

If $\mathbf{P}$ is the 2×2 covariance of the estimated position corresponding to the North and East directions, the projection of the covariance to calculate sigma (σ_L) can be calculated using

$$\sigma_L^2 = \sup_{\theta}\left([\cos(\theta) \quad \sin(\theta)]\mathbf{P}\begin{bmatrix}\cos(\theta)\\ \sin(\theta)\end{bmatrix}\right). \tag{32}$$

ACKNOWLEDGMENT

The authors would like to specifically acknowledge the support and guidance of Glenn Colby and Marie Lage regarding this work. The authors also acknowledge Shuwu Wu of Raytheon Company for the discussion regarding this work.

REFERENCES

[1] Minimum Aviation System Performance Standards for the Local Area Augmentation System Airborne Equipment.
RTCA document DO-245A, Dec. 2004.

[2] Hansen, J., Romrell, G., Nabaa, N., Andersen, R., Myers, L., and McCormick, J.
DARPA autonomous airborne refueling demonstration program with initial results.
In *Proceedings of the 19th International Technical Meeting of the Satellite Division of the Institute of Navigation ION GNSS 2006*, Fort Worth, TX, Sept. 2006.

[3] Khanafseh, S., Pervan, B., and Colby, G.
Carrier phse DGPS for autonomous irborne refueling.
In *Proceedings of the 2005 National Technical Meeting of the Institute of Navigation*, San Diego, CA, Jan. 2005.

[4] Dogra, S., Wright, J., and Hansen, J.
Sea-based JPALS relative navigation algorithm development.
In *Proceedings of the 18th International Technical Meeting of the Satellite Division of the Institute of Navigation ION GNSS 2005*, Long Beach, CA, Sept. 2005.

[5] Heo, M., Pervan, B., Pullen, S., Gautier, J., Enge, P., and Gebre-Egziabher, D.
Robust airborne navigation algorithm for SRGPS.
In *Proceedings of the IEEE/ION Position, Location, and Navigation Symposium* (PLANS '04), Monterey, CA, Apr. 2004.

[6] Kim, D., and Langley, R.
GPS ambiguity resolution and validation: Methodologies, trends and issues.
In *Proceedings of the 7th GNSS Workshop—International Symposium on GPS/GNSS*, Seoul, Korea, Nov. 2000.

[7] Pervan, B., and Chan, F. C.
System concepts for cycle ambiguity resolution and verification for aircraft carrier landings.
In *Proceedings of the 14th International Technical Meeting of the Satellite Division of the Institute of Navigation ION GPS 2001*, Salt Lake City, UT, Sept. 2001.

[8] Heo, M. B.
Robust carrier phase DGPS Navigation for Shipboard Landing of Aircraft.
Ph.D. dissertation, Illinois Institute of Technology, Chicago, IL, Dec. 2004.

[9] Khanafseh, S., Kempny, B., and Pervan, B.
New applications of measurement redundancy in high performance relative navigation systems for aviation.
In *Proceedings of the 19th International Technical Meeting of the Satellite Division of the Institute of Navigation ION GNSS 2006*, Fort Worth, TX, Sept. 2006.

[10] Teunissen, P.
GNSS ambiguity bootstrapping: Theory and application.
In *Proceedings of KIS2001, International Symposium on Kinematic Systems in Geodesy, Geomatics and Navigation*, Banff, Canada, 2001.

[11] Teunissen, P., Odijk, D., and Joosten, P.
A probabilistic evaluation of corrct GPS ambiguity resolution.
In *Proceedings of the 11th International Technical Meeting of the Satellite Division of the Institute of Navigation*, Nashville, TN, Sept. 1998.

[12] Hassibi, A., and Boyd, S.
Integer parameter estimation in linear models with application to GPS.
IEEE Transactions on Signal Processing, **46**, 11 (Nov. 1998).

[13] Teunissen, P., Joosten, P., and Tiberius, C.
Geometry-free ambiguity success rate in case of partial fixing.
In *Proceedings of the 1999 National Technical Meeting of the Institute of Navigation*, San Diego, CA, Jan. 1999.

[14] Misra, P., and Enge, P.
Global Positioning System Signals, Measurements, and Performance.
Lincoln, MA: Ganga-Jamuna Press, 2001.

[15] McGraw, G. A., and Young, R. S. Y.
Dual frequency smoothing DGPS performance evaluation studies.
In *Proceedings of the 2005 National Technical Meeting of the Institute of Navigation*, San Diego, CA, Jan. 2005.

[16] Minimum Operational Performance Standards for Global Positioning System/Wide Area Augmentation System Airborne Equipment.
RTCA document DO-229C, Nov. 2001, App. B.5.

Samer Khanafseh received a mechanical engineering degree in 2000 from Jordan University of Science and Technology, Irbid-Jordan and received M.S. and Ph.D. degrees in aerospace engineering at Illinois Institute of Technology, Chicago in 2003 and 2008, respectively.

In his Ph.D., he designed and implemented a high accuracy and integrity GPS based navigation architecture for autonomous airborne refueling of unmanned air vehicles. In that research, he developed a KC-135 tanker blockage model, provided flight test planning, support, and post processing, and developed a real time flight algorithms that were implemented onboard the UAV-surrogate in 2007 AAR fight test. Currently, he works as a research associate in the Navigation Lab in the same institute.

His research interests are focused on high accuracy navigation algorithms for close proximity applications such as Autonomous Air Refueling and autonomous shipboard landing, cycle ambiguity resolution, high integrity applications and robust estimation techniques.

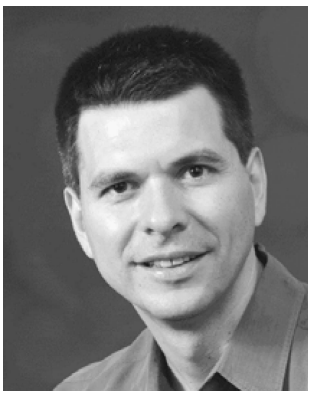

Boris Pervan received a B.S. from the University of Notre Dame in 1986, M.S. from the California Institute of Technology in 1987, and Ph.D. from Stanford University in 1996, all in aerospace engineering.

From 1987 to 1990, he was a systems engineer at Hughes Space and Communications Group responsible for mission analysis on commercial and government spacecraft programs. He was a research associate at Stanford from 1996 to 1998, serving as project leader for GPS Local Area Augmentation System (LAAS) research and development. He is now an Associate Professor of Mechanical and Aerospace Engineering at the Illinois Institute of Technology (IIT) in Chicago.

Dr. Pervan received the RTCA William E. Jackson Award (1996), the M. Barry Carlton Award from the IEEE Aerospace and Electronic Systems Society (1999), Sigma Xi Outstanding Research Award at IIT (2005), Excellence in Teaching awards at IIT (2002, 2005), the Albert Zahm Prize in Aeronautics at Notre Dame (1986), and the Guggenheim Fellowship at Caltech (1987). He is currently editor of the ION journal *Navigation*.